AGU PUBLICATIONS

Geophysical Research Letters

RESEARCH LETTER
10.1002/2014GL061895

Key Points:
- There are large deficiencies in the only century-long record of these storms
- The past 25 years have not produced detectable trends in storm numbers
- Improved monitoring of monsoon depressions and their activity is needed

Supporting Information:
- Readme
- Text S1
- Figure S1
- Figure S2
- Figure S3
- Figure S4
- Figure S5
- Figure S6

Correspondence to:
N. Y. Cohen,
naftalic@gmail.com

Citation:
Cohen, N. Y., and W. R. Boos (2014), Has the number of Indian summer monsoon depressions decreased over the last 30 years?, *Geophys. Res. Lett.*, *41*, 7846–7853, doi:10.1002/2014GL061895.

Received 17 SEP 2014
Accepted 28 OCT 2014
Accepted article online 30 OCT 2014
Published online 24 NOV 2014

Has the number of Indian summer monsoon depressions decreased over the last 30 years?

Naftali Y. Cohen[1] and William R. Boos[1]

[1] Department of Geology and Geophysics, Yale University, New Haven, Connecticut, USA

Abstract Monsoon depressions are cyclonic atmospheric vortices with outer radii near 1000 km that form within the larger-scale monsoon circulations of India and other regions. Recent studies have reported a downward trend in recent decades in the number of Indian summer monsoon depressions. In particular, the years 2002, 2010, and 2012 were noted for having the first summers, in over a century, in which no depressions formed. Here satellite and reanalysis data are used to document the existence of multiple storms in the summers of 2002, 2010, and 2012 that meet traditional criteria for classification as monsoon depressions. Furthermore, the number of extreme synoptic events occurring each summer over the Bay of Bengal is estimated from satellite scatterometers and exhibits no statistically significant trend over the last three decades. These results raise questions about the validity of previously claimed large trends in monsoon depression activity in the Indian summer monsoon.

1. Introduction

Precipitation in the summer monsoon season accounts for more than 80% of India's annual rainfall and is crucial for the region's agriculture and economy [*Ding and Sikka*, 2006]. A large fraction of this summer precipitation is produced by vortices with outer radii of about 1000 km that typically form over the Bay of Bengal [*Sikka*, 1977] (Figure 1a). Severe precipitation in these storms, which commonly reaches 40–50 mm d^{-1}, causes floods and great destruction in populous regions [*Lau and Kim*, 2012; *Houze et al.*, 2011; *Boos et al.*, 2014].

Intense occurrences of these synoptic-scale storms are commonly classified as monsoon depressions: cyclonic vortices with peak surface wind speeds of 8.5–13.5 m s^{-1} and surface pressure minima 4–10 hPa below that of surrounding regions [*India Meteorological Department*, 2011; *Ajayamohan et al.*, 2010]. Weaker vortices with similar horizontal scale are called monsoon lows, and stronger vortices are called deep depressions or cyclonic storms. Hereafter, we refer to any synoptic-scale cyclonic vortex with intensity higher than that of a monsoon low as a monsoon depression (MD); this is done both for simplicity and to ease comparison between different data sets (as described below). Monsoon depressions typically have positive vorticity in the lower to middle troposphere and a warm-over-cold core that extends to the upper troposphere and tilts to the southwest with height. Maximum precipitation occurs southwest of the vortex center [*Sikka*, 1977; *Ding and Sikka*, 2006]. After formation, Indian monsoon depressions propagate to the west-northwest at an average speed of about 2 m s^{-1} and have a lifetime of about 3–5 days [*Ding and Sikka*, 2006].

Records from the India Meteorological Department (IMD) show that an average of about six monsoon depressions formed each summer (June–September) in the Indian region (5–30°N and 50–100°E) over the last century. Recent analyses of these records over the Bay of Bengal domain (5–27°N and 70–100°E, marked with a black box in Figure 1a) have revealed a statistically significant decreasing trend in the number of depressions (Figures 1b and 2) but an increase in the number of weaker storms since the midtwentieth century [*Kumar and Dash*, 2001; *Dash et al.*, 2004, 2007; *Sikka*, 2006]. The increased number of weak storms has been argued to dominate and produce an upward trend in overall synoptic activity that is accompanied by an increase in extreme rain events over that same period [*Goswami et al.*, 2006; *Ajayamohan et al.*, 2010; *Singh et al.*, 2014], with some disagreement in the analyzed precipitation trends [*Ghosh et al.*, 2012]. The years of 2002, 2010, and 2012 were noted for having the first summers, in over a century of record keeping, in which no depressions formed in the Indian monsoon. A number of studies have associated the downward trend in monsoon depressions with climate change [*Goswami et al.*, 2006; *Turner and Annamalai*, 2012; *Prajeesh et al.*, 2013], while others have argued that enhanced concentrations of atmospheric aerosols suppress the intensification of monsoon lows into monsoon depressions [*Krishnamurti et al.*, 2013].

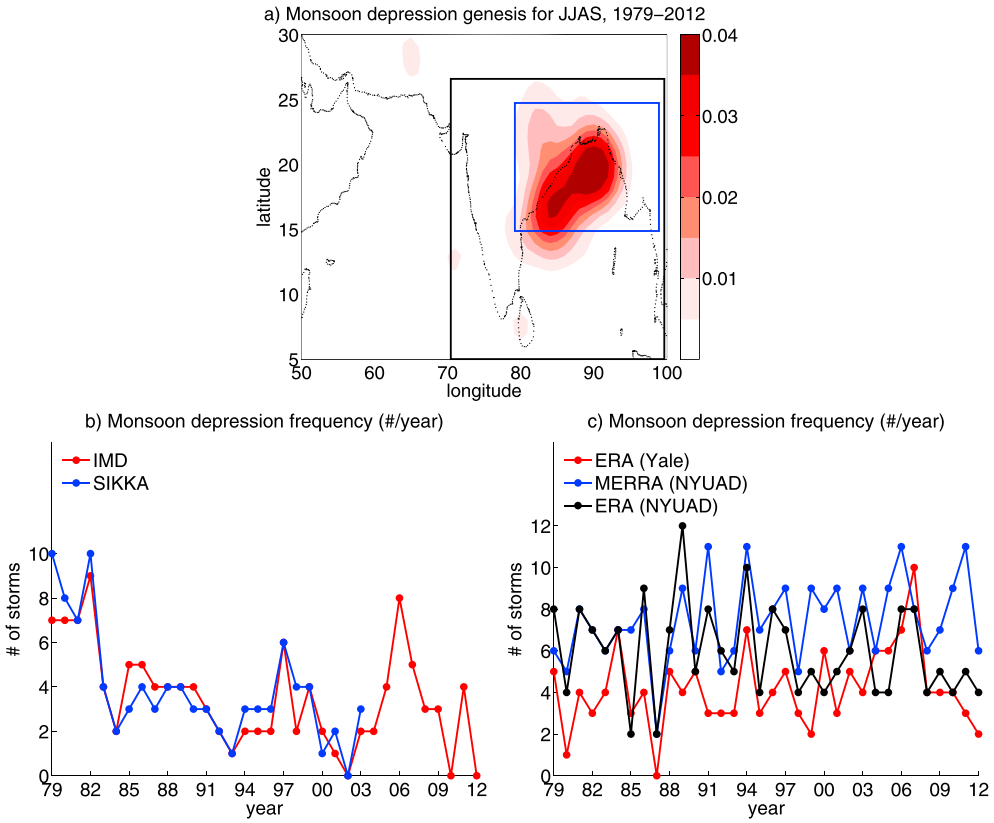

Figure 1. Monsoon depression genesis distribution and frequency. (a) The smoothed number of monsoon depression genesis points per square degree (roughly 12,000 km^2), in the Yale data set, per summer season (June–September) in the Indian domain (5–30°N, 50–100°E) during 1979–2012. The genesis points were smoothed using a Gaussian filter with 1.75° standard deviations. (b and c) The summer monsoon depression count in the Bay of Bengal (5–27°N, 70–100°E; the black box in Figure 1a) as a function of the year (1979–2012). Figure 1b shows the IMD data (red) and Sikka data (blue), and Figure 1c shows ERA-Interim data using the Yale (red) and the NYUAD (black) tracking algorithms, as well as MERRA data using the NYUAD (blue) tracking algorithms. Nonlinear Poisson regression fits [*Solow and Moore*, 2000; *Wilks*, 2011] to the data sets are shown in Figure 2 and Table S1 in the supporting information. The blue box in Figure 1a marks the region of analysis used in Figure 4.

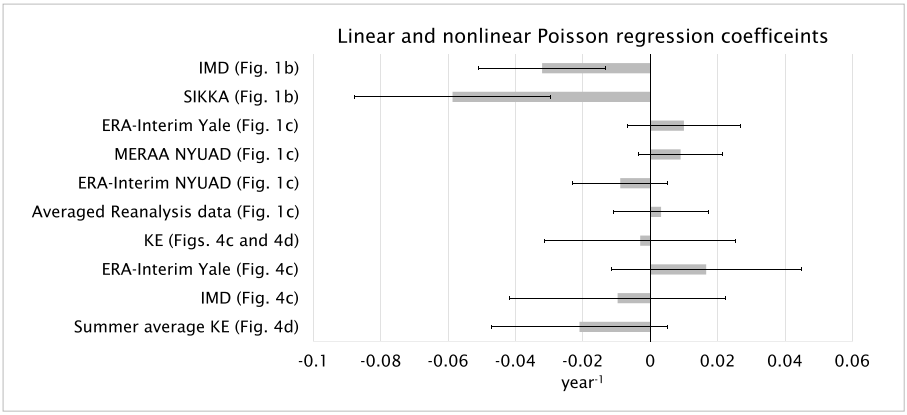

Figure 2. Linear regression and nonlinear Poisson regression fits [*Solow and Moore*, 2000; *Wilks*, 2011] to the data sets presented in Figures 1b, 1c, 4c, and 4d. Here only the slope coefficients (i.e., the gradient of the regression fits) are shown, and error bars represent the 95% confidence interval for these coefficients. Units are year^{-1}. More information, including the *y* intercepts, can be found in the supporting information to the text (Table S1). Linear regression was used for the summer mean KE and Poisson regression for all other time series.

Here we question the existence of a trend in the number of Indian summer MDs. We demonstrate that errors exist in the IMD data set, and we fail to detect a trend in several other data sets of Indian MD activity. However, all of those alternate data sets have issues that may bias their long-term trends, so we do not definitively answer the question posed in the title of this paper. A robust, definitive, decades-long record of MD activity may require a large effort by teams of researchers examining historical meteorological observations, such as is ongoing for tropical cyclone best track data sets; this is beyond the scope of this paper.

2. Depressions in Reanalysis Data

The IMD records of monsoon depression counts date back to the late nineteenth century, when weather charts were drawn by hand based on observations received by telegraph, and extend through the beginning of the satellite era to the present [*India Meteorological Department*, 2011]. Methods of identifying and tracking storms changed throughout that period together with the observing network itself, with satellite data used in storm detection in recent decades. Some studies have reanalyzed the tracks of Indian monsoon synoptic vortices using manual identification from IMD weather charts [*Mooley and Shukla*, 1987; *Sikka*, 2006, hereafter referred to as the Sikka dataset] and have also found a statistically significant decreasing trend in depression counts (Figures 1b and 2). The IMD and Sikka data sets are highly correlated and exhibit only minor deviations. The publicly available IMD record does not distinguish between "depressions" and "deep depressions," which is why we include all storms with intensities equal to or greater than that of a monsoon depression in our analysis; this also eliminates the possibility that storm counts could differ if one algorithm classifies a storm as a "depression" and another classifies it as a "deep depression" or "cyclonic storm."

Investigators at Yale University [*Hurley and Boos*, 2014] recently used an automated tracking algorithm to identify trajectories of relative vorticity maxima in the latest reanalysis of the European Centre for Medium-Range Weather Forecasts (ERA-Interim) and categorized those vortices by intensity in ways consistent with traditional definitions used by the IMD. In short, the algorithm uses a feature-tracking scheme [*Hodges*, 1995, 1998] to identify and track 850 hPa relative vorticity maxima that exceed 1×10^{-5} s^{-1} in magnitude. Vortices are also required to have a sea level pressure anomaly, relative to a 21 day running mean, with amplitude of at least 4 hPa and a surface wind speed of at least 8.5 m s^{-1}, consistent with the aforementioned criteria for depressions. These pressure and wind criteria must be satisfied within 500 km of the relative vorticity maximum and must occur simultaneously during at least one 6 h period along the track.

This track data set (hereafter referred to as the Yale data set), at 6-hourly temporal and 0.75° spatial resolution, has a distribution of genesis points for monsoon depressions similar to that seen in IMD data [*Mooley and Shukla*, 1989], with most depressions forming over the northwest Bay of Bengal (Figure 1a). However, the Yale data set shows that multiple depressions formed during the summers of 2002, 2010, and 2012, years which were remarkable for lacking any summer monsoon depression in the IMD record (Figure 1c). No statistically significant long-term trend exists in the Yale data set (Figure 2), although this finding is of questionable value because changes in the global observing system can bias long-term trends in reanalysis products [e.g., *Bengtsson et al.*, 2004]. For example, the early part of reanalysis-based storm count time series might have a larger error of unknown sign because less satellite data were assimilated in the early part of those records. Nevertheless, the identification of multiple storms in 2002, 2010, and 2012—years in which abundant satellite data were assimilated by ERA-Interim—prompts us to ask whether the IMD data set underestimates MD counts, at least in recent years.

We examine two additional records of Indian MD counts derived by investigators at New York University Abu Dhabi (and hereafter referred to as the NYUAD data sets). These records are also based on reanalysis data but use a different objective tracking algorithm that relies only on surface pressure to identify Indian MDs. As described in V. Praveen et al. (Role of mid-tropospheric stability in the simulation of monsoon low pressure systems, submitted to *Journal of Climate*, 2014), this method was designed to mimic the manual detection and tracking performed by *Sikka* [2006] using daily surface pressure charts. Climatological low-pressure features, such as desert heat lows and the mean monsoon trough, are not included in the resulting data set. This method was applied to both ERA-Interim data and the Modern-Era Retrospective analysis for Research and Applications (MERRA) [*Rienecker et al.*, 2011].

The NYUAD algorithm, when applied to both ERA-Interim and MERRA, also yields multiple monsoon depressions over the Bay of Bengal during the summers of 2002, 2010, and 2012 (Figure 1c). The NYUAD analysis of both ERA-Interim and MERRA show no trend (Figure 2). There is a positive, statistically significant correlation between the various reanalysis products (0.4 using the Pearson correlation measure), but correlations between the reanalysis products and the IMD data are weak and insignificant. Disagreements between these time series may arise from differences in the underlying data sets or from differences in the MD identification algorithms. Storm counts are known to deviate greatly (e.g., by an order of magnitude for the case of tropical cyclones detected in global models) depending on the algorithm used for the objective tracking [e.g., *Suzuki-Parker*, 2012]. Nevertheless, it is important to note that neither of the NYUAD records have a single year in which zero MDs formed during summer over the Bay of Bengal, lending support to the idea that the IMD data set might be missing storms in the most recent decades.

3. Missing Monsoon Depressions

To determine if the depressions found in the reanalysis data during the summers of 2002, 2010, and 2012 are real and not artifacts of the identification algorithms or reanalysis products, we examine sea level pressure and surface wind from ERA-Interim, in addition to satellite estimates of precipitation and oceanic surface wind. Satellite data were obtained from the following sources:

1. Daily precipitation estimates were obtained from the Tropical Rainfall Measuring Mission (TRMM) satellite that was launched in November 1997. This data set uses several spaceborne rainfall-measuring instruments, including a precipitation radar, to estimate the rainfall distribution over land and ocean with 3-hourly temporal resolution and 0.25° × 0.25° spatial resolution. Spatial coverage extends from 50°S to 50°N.
2. Ocean surface wind speeds were obtained from the Special Sensor Microwave Imager (SSMI) radiometers carried by a series of eight satellites that began their near-polar orbits in 1987 [*Wentz*, 2013]. These satellites make over 14 orbits daily and cross the equator at roughly the same local solar time each day. Drift, due to orbit degradation, in the equatorial crossing time for each satellite varies up to about 3 h. Satellites with overlapped functionality differ in equatorial crossing time by up to about 3 h over their operational lifetime. Thus, we expect diurnal sampling biases to be of a minor effect. Wind speeds derived from these satellites have 0.25° spatial resolution. We analyzed 3 day average wind speeds derived from satellites F08, F10, F11, F13, F14, F15 (values after August 2006 were discarded due to a calibration problem), F16, and F17. Data are mostly continuous, with gaps primarily due to Sun glint, rain, radio frequency interference, sea ice, or land. We further smoothed the wind speeds by averaging over the available operational satellites.
3. Daily surface vector winds at about 0.25° spatial resolution were obtained from QuikScat and WindSat scatterometers. QuikScat is a satellite in Sun-synchronous low-Earth orbit carrying an active microwave instrument and was launched in June 1999 and operated until November 2009. WindSat was launched on 6 January 2003 (and still operates) aboard the Coriolis satellite in a near-polar low-Earth orbit. Both satellites complete about 14 orbits per day.

Figure 3 shows various fields from these data sets for one synoptic-scale storm per summer in 2002, 2010, and 2012, as identified in both the Yale and NYUAD data sets. All three of these vortices should be classified as monsoon depressions based on either the maximum surface wind speed or sea level pressure criteria traditionally used by the IMD. Surface vector winds obtained from both reanalysis and satellite data show that in addition to satisfying surface wind speed criteria, these storms had cyclonic surface flow as expected for monsoon depressions. Although circular flow is not always visible in the scatterometer winds, particularly when the vortex center is in coastal or continental regions, heavy precipitation (>40 mm d^{-1}) always occurs within a typical radius of the storm center. In the supporting information (Figures S1–S3) we show the same fields for five more depressions that occurred during the summers of 2002, 2010, and 2012, confirming that multiple depressions are missing from the IMD data set in recent years.

4. Extreme Synoptic Activity Estimated From Satellite Data

While it is possible that the fraction of monsoon depressions missing from the IMD data set is constant over time, variations in this fraction could introduce a bias to long-term trends inferred from the IMD storm

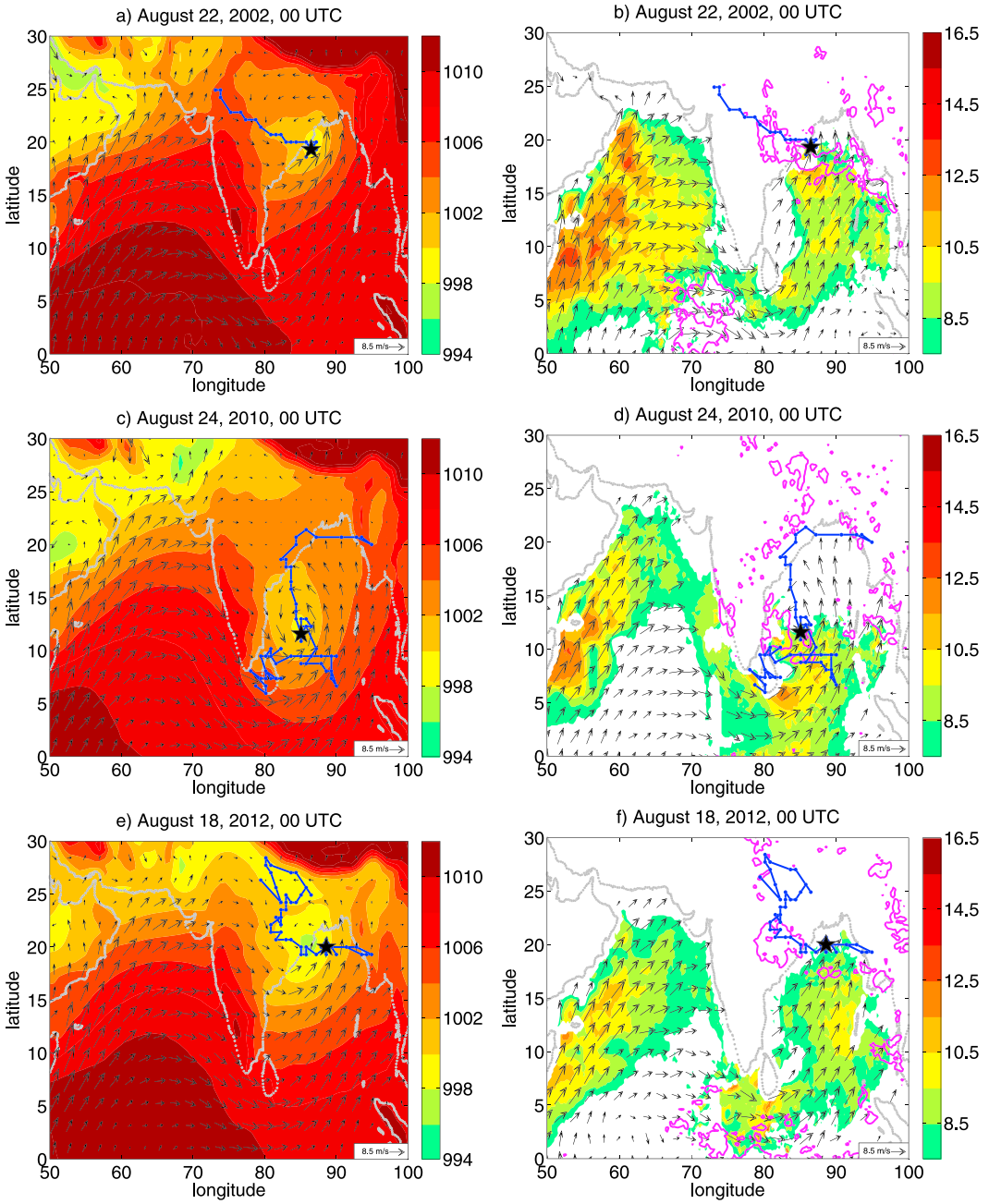

Figure 3. Three monsoon depressions observed in the Yale and NYUAD data sets during the summers of 2002, 2010, and 2012. In all panels storm tracks (from the Yale data set) are shown by blue lines with vortex center marked with a black star. (a, c, and e) ERA-Interim sea level pressure (in hPa) is shaded, and black arrows show the ERA-Interim surface wind vector field. (b, d, and f) SSMI surface wind speed is shaded, while arrows show surface wind vector from QuikSCAT (Figure 3b) and WindSat (Figures 3d and 3f) scatterometers. The thick magenta contour shows the 40 mm d^{-1} daily TRMM precipitation. Precipitation, winds, and the vortex center position are shown for the dates indicated above each panel.

counts. We would ideally like a decades-long, continuous observational record of MD activity that does not vary over time in its spatial coverage or calibration. Here we examine ocean surface wind speeds estimated by SSMI satellite scatterometers that have been in operation since 1987. These wind speeds have been filtered, by removing a 21 day moving average, to produce an estimate of the kinetic energy (KE) of synoptic-scale disturbances over the main genesis region for monsoon depressions (15–25°N and 80–100°E, marked with a blue box in Figure 1a). This smaller domain is used here in order to focus on the region

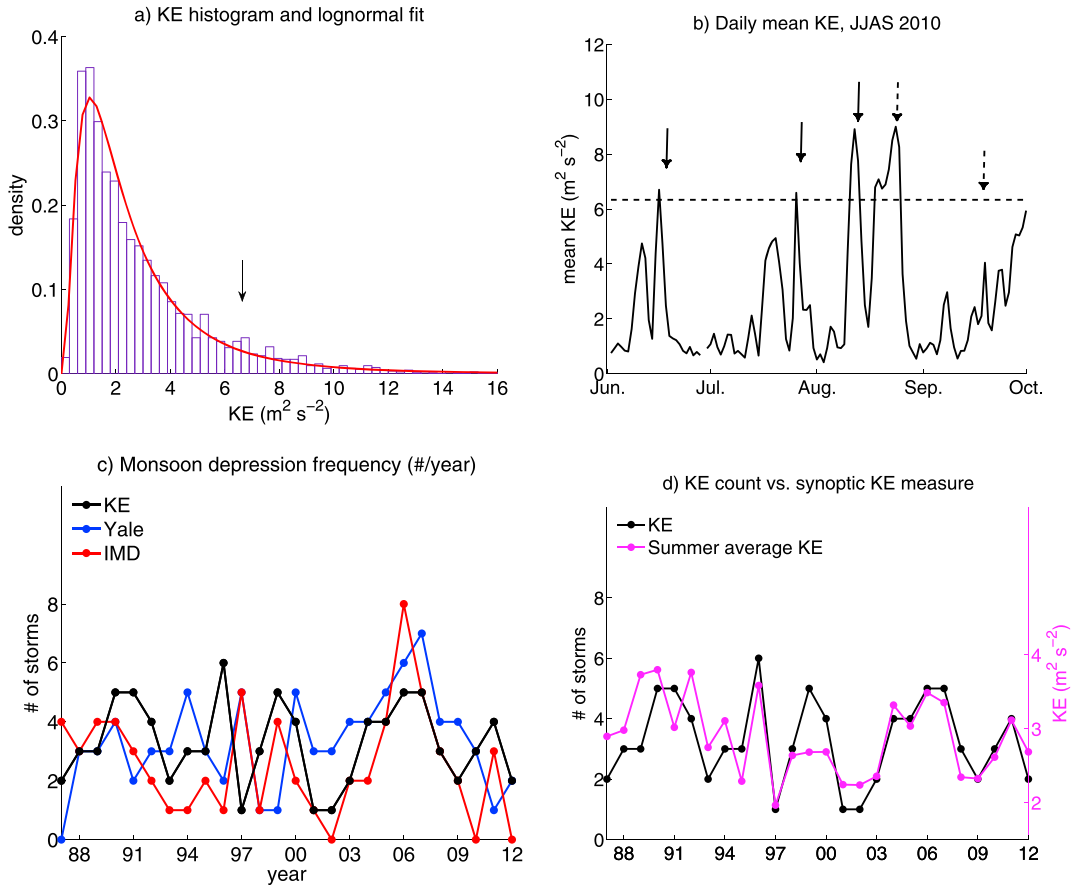

Figure 4. Analysis of ocean surface wind observations over the main genesis region of the Bay of Bengal domain (15–25°N and 80–100°E). (a) A histogram of the Bay of Bengal synoptic KE for 1987–2012 derived from SSMI scatterometer ocean surface wind speeds. The lognormal probability density fit is shown in red, and the 90th percentile is marked by the small black arrow. (b) The synoptic KE as a function of time for the summer of 2010, with the 90th percentile threshold for extreme events marked by the dashed line. Arrows correspond to monsoon lows (dashed) and monsoon depressions (solid) that took place roughly around the same time in the Bay of Bengal domain. (c) The number of extreme events in the domain using the synoptic KE proxy for storm counts (black) as well as the Yale (blue) and IMD (red) monsoon depression counts during the summers of 1987–2012. (d) Comparison of the KE count (black, same as in Figure 4c) with the summer average synoptic KE (magenta). Linear and nonlinear Poisson regression fits [*Solow and Moore*, 2000; *Wilks*, 2011] to the data sets are shown in Figure 2 and Table S1.

of highest MD activity and minimize the contribution of variability in more remote regions that may be associated with other phenomena.

The area integral of this KE (hereafter referred to as the synoptic KE) is approximately described by a lognormal probability distribution (Figure 4a), indicating that the Bay of Bengal is largely calm on synoptic timescales but has a wide range of extreme events. The goodness of the lognormal fit, relative to other probability distributions, was verified using the negative of the log likelihood and Bayesian information criterion [*Wilks*, 2011].

While monsoon depressions cannot be unambiguously identified using only scalar oceanic surface wind speeds, the existence of depressions over the ocean is expected to project onto the synoptic-scale ocean surface wind variability. Changes in the number of depressions might then be deduced from changes in this synoptic-scale ocean surface wind variability. This motivates our use of the number of synoptic KE extremes occurring each summer as a proxy for monsoon depression activity within the oceanic domain of the Bay of Bengal. The threshold used to define extreme events was chosen, simply, as the 90th percentile in accumulated probability of the synoptic KE (marked by an arrow in Figure 4a). Furthermore, an event is defined if and only if it is followed by five consecutive days (a rough monsoon depression lifetime) [*Sikka*, 2006; *Hurley*

and Boos, 2014] of values below the 90th percentile (results were verified to be insensitive to small variations in this time interval). Time series of the synoptic KE show a decent correspondence between events that exceeded the 90th percentile and individual monsoon depressions in the Yale data set (e.g., Figure 4b). However, some depressions do not produce synoptic KE extremes because they originate over land or in coastal regions, while other storms that are too weak to be classified as depressions produce synoptic KE extremes because of their larger size (analyses of the summers of 2002 and 2012 are shown in Figure S4 in the supporting information).

By counting the number of synoptic KE peaks in each summer that exceed the 90th percentile threshold, we obtain a yearly time series for the number of extreme synoptic events over the Bay of Bengal. The correlation of this time series, over the smaller domain, with IMD counts is moderate but statistically significant (0.4 using Kendall/Spearman correlation measures), but the correlation with Yale counts is low. Regardless, it confirms that multiple extreme synoptic events occurred during the summers of 2002, 2010, and 2012 (Figure 4c). This finding is robust to changes in the threshold used to define a synoptic KE extreme (see Figure S5 in the supporting information). Robustness is also indicated by the high correlation (0.6/0.7 using Kendall/Spearman correlation measures) of the KE-based count with a more straightforward summer average of the synoptic KE (Figure 4d).

During the period of 1987–2012, no statistically significant trend exists in the number of synoptic KE extremes or in the number of monsoon depressions in the Yale or IMD data sets (Figures 4c and 2). There is a weak downward linear trend in the summer mean synoptic KE, but this is not statistically significant (Figure 2). Examination of the full IMD time series over the Bay of Bengal domain (see Figure S6 in the supporting information) shows that an 11 year moving average of monsoon depression count remained at or above seven per summer from the 1920s through 1980 then underwent a steep decline over 20 years to about half that value. If the decline in storm counts occurred almost entirely before 1987, then one could not expect to see a significant trend in any of the time series shown in Figure 4c, even in the IMD time series. Establishing the existence of a long-term trend in depression counts would then require data from the pre-satellite and early satellite era, a time when oceanic disturbances with relatively disorganized convection (such as monsoon depressions) may have been poorly observed.

5. Summary and Conclusions

In summary, our results demonstrate the existence of multiple Indian MDs during summers in which the IMD data set contains no such storms. This indicates possible errors in that data set, on which previous claims of large trends in monsoon depression activity have been based. Unfortunately, reanalysis data sets may not be viable alternate sources for trends in MD counts because of temporal changes in the observing network. Nevertheless, we note that no trends could be found in two reanalysis products analyzed with two different storm identification algorithms. Given the hydrological importance of synoptic activity in the world's monsoon regions and the vulnerability of societies in those regions to hydrological change [*Yoon and Chen*, 2005; *Berry et al.*, 2012; *Hurley and Boos*, 2014], this indicates a need for improved monitoring of monsoon depressions and more in-depth study of possible trends in their activity. Here one 30–year long satellite data set is used to show that there is no large, statistically significant trend in the synoptic-scale variability of ocean surface winds over the Bay of Bengal. Similar analyses of other long-term, continuous, uniformly calibrated, records of meteorological data (e.g., surface weather stations or balloon sounding data) are needed to validate the existence of trends in monsoon depression activity.

Acknowledgments

We thank V. Praveen, S. Sandeep, and R.S. Ajayamohan from the Center for Prototype Climate Modeling, New York University Abu Dhabi, UAE, for providing their ERA and MERRA monsoon depression tracking data. We also thank R.S. Ajayamohan and two anonymous reviewers for useful comments and discussion. We thank Sarah Ditchek for providing an electronic version of the Sikka data. Both authors acknowledge support by Office of Naval Research Young Investigator Program award N00014-11-1-0617 and National Science Foundation award AGS-1253222. The India Meteorological Department record of monsoon depression tracks was downloaded from the IMD website at www.imd.gov.in. The ERA-Interim reanalysis was obtained from the Research Data Archive that is maintained by the Computational and Information Systems Laboratory at the National Center for Atmospheric Research (NCAR). NCAR is sponsored by the National Science Foundation. The data are available at http://rda.ucar.edu. TRMM daily accumulated rainfall product (version 7 of the 3B42) was obtained from the NASA Goddard Space Flight Center at http://precip.gsfc.nasa.gov. The Yale data set is publicly available at http://earth.geology.yale.edu/depressdata/. SSMI, QuikScat, and WindSat scatterometer data are produced by Remote Sensing Systems. The data are sponsored by the NASA Earth Science MEaSUREs Program and DISCOVER Project, NASA Ocean Vector Winds Science Team, and NASA Earth Science Physical Oceanography Program. The data are available at http://www.remss.com/.

The Editor thanks two anonymous reviewers for their assistance in evaluating this paper.

References

Ajayamohan, R. S., W. J. Merryfield, and V. V. Kharin (2010), Increasing trend of synoptic activity and its relationship with extreme rain events over Central India, *J. Clim.*, *23*, 1004–1013.

Bengtsson, L., S. Hagemann, and K. I. Hodges (2004), Can climate trends be calculated from reanalysis data?, *J. Geophys. Res.*, *109*, D11111, doi:10.1029/2004JD004536.

Berry, G. J., M. J. Reeder, and C. Jakob (2012), Coherent synoptic disturbances in the Australian Monsoon, *J. Clim.*, *25*(24), 8409–8421.

Boos, W. R., J. V. Hurley, and V. S. Murthy (2014), Adiabatic westward drift of Indian monsoon depressions, *Q. J. R. Meteorol. Soc.*, doi:10.1002/qj.2454.

Dash, S., R. Jenamani, S. Kalsi, and S. Panda (2007), Some evidence of climate change in twentieth-century India, *Clim. Change*, *85*(3-4), 299–321.

Dash, S. K., J. R. Kumar, and M. S. Shekhar (2004), On the decreasing frequency of monsoon depressions over the Indian region, *Curr. Sci.*, *86*, 1404–1411.

Ding, Y., and D. Sikka (2006), Synoptic systems and weather, in *The Asian Monsoon*, edited by B. Wang, pp. 131–201, Springer, Berlin.
Ghosh, S., D. Das, S.-C. Kao, and A. R. Ganguly (2012), Lack of uniform trends but increasing spatial variability in observed Indian rainfall extremes, *Nat. Clim. Change*, *2*, 86–91.
Goswami, B. N., V. Venugopal, D. Sengupta, M. S. Madhusoodanan, and P. K. Xavier (2006), Increasing trend of extreme rain events over India in a warming environment, *Science*, *314*, 1442–1445.
Hodges, K. I. (1995), Feature tracking on the unit sphere, *Mon. Weather Rev.*, *123*, 3458–3465.
Hodges, K. I. (1998), Feature-point detection using distance transforms: Application to tracking tropical convective complexes, *Mon. Weather Rev.*, *126*, 785–795.
Houze, R., K. Rasmussen, S. Medina, S. Brodzik, and U. Romatschke (2011), Anomalous atmospheric events leading to the summer 2010 floods in Pakistan, *Bull. Am. Meteorol. Soc.*, *92*(3), 291–298.
Hurley, J. V., and W. R. Boos (2014), A global climatology of monsoon low-pressure systems, *Q. J. R. Meteorol. Soc.*, doi:10.1002/qj.2447.
India Meteorological Department (2011), Tracks of cyclones and depressions over North Indian Ocean (from 1891 onwards), *Tech. Note Version 2.0*, Cyclone Warning and Research Centre India Meteorological Department Regional Meteorological Centre, Chennai, India.
Krishnamurti, T., A. Martin, R. Krishnamurti, A. Simon, A. Thomas, and V. Kumar (2013), Impacts of enhanced CCN on the organization of convection and recent reduced counts of monsoon depressions, *Clim. Dyn.*, *41*, 117–134.
Kumar, J. R., and S. K. Dash (2001), Interdecadal variations of characteristics of monsoon disturbances and their epochal relationships with rainfall and other tropical features, *Int. J. Climatol.*, *21*, 759–771.
Lau, K. M., and K.-M. Kim (2012), The 2010 Pakistan flood and Russian heatwave: Teleconnection of hydrometeorologic extremes, *J. Hydrometeorol.*, *13*, 392–403.
Mooley, D. A., and J. Shukla (1987), Characteristics of the westward-moving summer monsoon low pressure systems over the Indian region and their relationship with the monsoon rainfall, Department of Meteorology, Center for Ocean-Land-Atmosphere Interactions, Univ. of Maryland, College Park, Md.
Mooley, D. A., and J. Shukla (1989), Main features of the westward-moving low pressure systems which form over the Indian region during the summer monsoon season and their relation to the monsoon rainfall, *Mausam*, *40*, 137–152.
Prajeesh, A. G., K. Ashok, and D. V. B. Rao (2013), Falling monsoon depression frequency: A Gray-Sikka conditions perspective, *Sci. Rep.*, *3*, 2989, doi:10.1038/srep02989.
Rienecker, M. M., et al. (2011), MERRA: NASA's Modern-Era Retrospective Analysis for Research and Applications, *J. Clim.*, *24*(14), 3624–3648.
Sikka, D. (1977), Some aspects of the life history, structure and movement of monsoon depressions, *Pure Appl. Geophys.*, *115*, 1501–1529.
Sikka, D. (2006), A study on the Monsoon Low Pressure systems over the Indian region and their relationship with drought and excess monsoon season rainfall, *COLA Tech. Rep. 217*, 61 pp., Center for Ocean-Land-Atmosphere Studies, Calverton, Md.
Singh, D., M. Tsiang, B. Rajaratnam, and N. S. Diffenbaugh (2014), Observed changes in extreme wet and dry spells during the South Asian summer monsoon season, *Nat. Clim. Change*, *4*, 456–461.
Solow, A. R., and L. Moore (2000), Testing for a trend in a partially incomplete hurricane record, *J. Clim.*, *13*(20), 2293–2305.
Suzuki-Parker, A. (2012), *Uncertainties and Limitations in Simulating Tropical Cyclones*, Springer, Berlin.
Turner, A. G., and H. Annamalai (2012), Climate change and the South Asian summer monsoon, *Nat. Clim. Change*, *2*, 587–595.
Wentz, F. J. (2013), SSM/I version-7 calibration report, *RSS Tech. Rep. 011012*, Remote Sensing Systems, Santa Rosa, Calif.
Wilks, D. (2011), *Statistical Methods in the Atmospheric Sciences*, Acad. Press, New York.
Yoon, J., and T. Chen (2005), Water vapor budget of the Indian monsoon depression, *Tellus A*, *57*(5), 770–782.

Supporting Information for "Has the number of Indian summer monsoon depressions decreased over the last thirty years?"

Naftali Y. Cohen and William R. Boos

Department of Geology and Geophysics, Yale University, New Haven, Connecticut

Corresponding author: Naftali Y. Cohen, Department of Geology and Geophysics, Yale University, P. O. Box 208109, New Haven, CT 06520-8109. E-mail: naftali.cohen@yale.edu

Introduction

This document presents supporting material to the main text.

Trend estimates (Fig. 2) are obtained using nonlinear Poisson regression which is particularly appropriate for count data with non-negative integers (*Solow and Moore* [2000]; *Wilks* [2011]). In addition, the superiority of the nonlinear fit over the linear fit was verified using the deviance measure. The deviance in nonlinear regression fits was found to be about three times smaller than in linear regression fits. The regression fits are shown in Supplemental Table 1. The standard errors of each fit's coefficients are shown parenthetically below the coefficients themselves (multiply by 1.96 to get the 95% confidence interval). For the time averaged synoptic kinetic energy (Fig. 4d) we used a simple linear regression [*Wilks*, 2011], as it is not count data.

Supplemental Figs. 1-3 complement Fig. 3 of the main text by showing the details of five additional monsoon depressions that formed over the Indian domain during the summer monsoon seasons of 2002, 2010 and 2012. These tracks were obtained from the Yale dataset, which was based entirely on ERA-Interim data, but the NYUAD datasets (based on ERA-Interim and MERRA using a different tracking algorithm) as well as the satellite-derived estimates of surface wind speeds and precipitation support classification of these disturbances as monsoon depressions. For example, scatterometer surface wind speeds easily exceed 8.5 m s^{-1} near the 850 hPa vortex center, and the scatterometer surface wind vectors show cyclonic curvature around the storm center in most cases (although in some cases the proximity of the vortex centers to the coast makes it difficult to unambiguously identify circular flow from oceanic winds alone). In addition, satellite and

gauge precipitation measurements show intense precipitation within the typical radius from the storm center.

It is possible that monsoon depressions that are missing from the IMD dataset were classified by the IMD as lows. We have examined the IMD Monsoon reports for 2010 and 2012 (*Tyagi et al.* [2011]; *Pai and Bhan* [2013]; 2002 is not available from the IMD website) and found that all of the storms for those years that are shown in Fig. 3 and Supp. Figs. 1-3 are indeed listed by the IMD as "low pressure areas" or "well-marked low pressure areas". Most are listed as having cyclonic circulation extending up to mid-tropospheric levels.

Supplemental Fig. 4 complements Fig. 4b of the main text by showing the synoptic KE count over the main genesis region of the Bay of Bengal domain (15-25°N and 80-100°E) as a function of time for the summers of 2002 and 2012 using SSM/I scatterometer data. Extreme events, our satellite-derived proxy for monsoon depressions, are defined when the synoptic KE exceeds its 90th percentile (marked by the dashed line). Arrows in the figures correspond to lows and depressions that occurred roughly around the same time according to the Yale dataset.

In the main text we presented a sensitivity test for the robustness of this synoptic KE threshold (see Fig. 4d). Supplemental Fig. 5 shows a second sensitivity test for the synoptic KE threshold. The solid black line in panel (a) shows how the summer mean synoptic KE storm count (using SSM/I scatterometer data for 1987-2012) varies as a function of the synoptic KE threshold. Clearly, as the threshold is raised fewer extreme events are identified. The dashed lines correspond to the summer mean monsoon

depression counts in the Yale (blue) and IMD (red) datasets. Identifying the cross-cutting points with the solid black line allows us to tune the synoptic KE threshold so that the synoptic KE count will yield the same summer mean monsoon depression count, for 1987-2012, as in the Yale or IMD datasets. Panel (b) shows time series of summer synoptic KE extremes using these two thresholds. The key point here is that either threshold produces multiple extreme events during the summers of 2002, 2010 and 2012. In addition, neither threshold provides evidence for a statistically significant decreasing trend in the extreme KE activity in the summer over the Bay of Bengal since 1987.

Lastly, Supplemental Fig. 6 shows the IMD summer monsoon depression count over the Bay of Bengal (5-27°N, 70-100°E) since 1891, together with an 11-year moving average of this quantity. The moving average remains at or above 5 storms per summer from the 1920s through the 1980s, then declines steeply over the next two decades. Definitive proof or disproof of the existence of this decline thus requires examination of storm counts before and in the very early part of the satellite era, before the availability of the satellite scatterometer record. This may be a difficult task, given that monsoon depressions have relatively weak surface pressure anomalies and relatively disorganized cloud patterns (e.g. compared to tropical cyclones).

References

Pai, D., and S. Bhan (2013), Monsoon 2012–a report, *Meteorological monographs (available from India Meteorological Department, New Delhi)*.

Solow, A. R., and L. Moore (2000), Testing for a trend in a partially incomplete hurricane record., *Journal of climate*, *13*(20).

Tyagi, A., A. Mazumdar, and D. Pai (2011), Monsoon 2010–a report, *Meteorological monographs (available from India Meteorological Department, New Delhi)*.

Wilks, D. (2011), *Statistical Methods in the Atmospheric Sciences*, Academic Press.

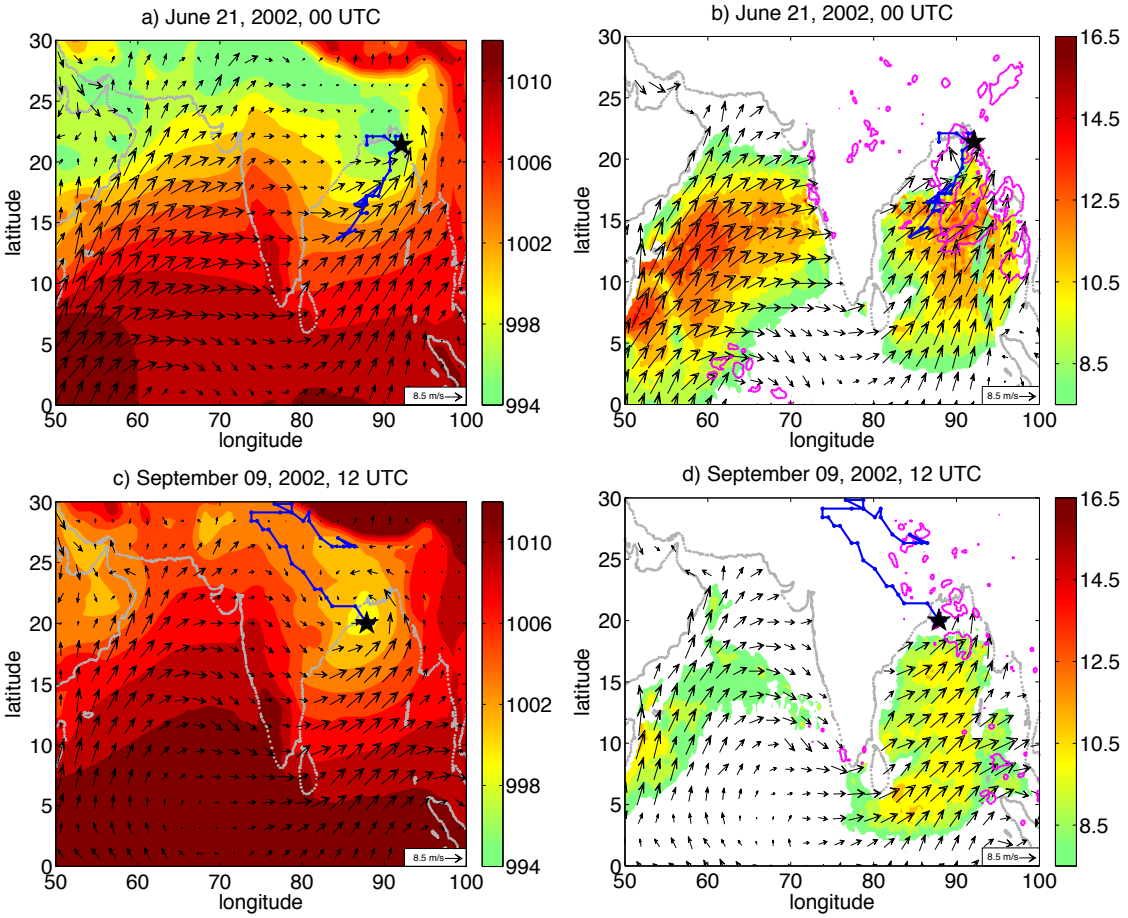

Supplemental Fig. 1 – Two monsoon depressions observed in the Yale and NYUAD datasets during the summer of 2002. In all panels storm tracks (from the Yale dataset) are shown by blue lines with vortex center marked with a black star. Left column: ERA-Interim sea-level pressure (in hPa) is shaded and black arrows show the ERA-Interim surface wind vector field. Right column: SSM/I surface wind speed is shaded, while arrows show surface wind vector from QuikSCAT scatterometer. The thick magenta contour shows the 40 mm day^{-1} daily TRMM precipitation.

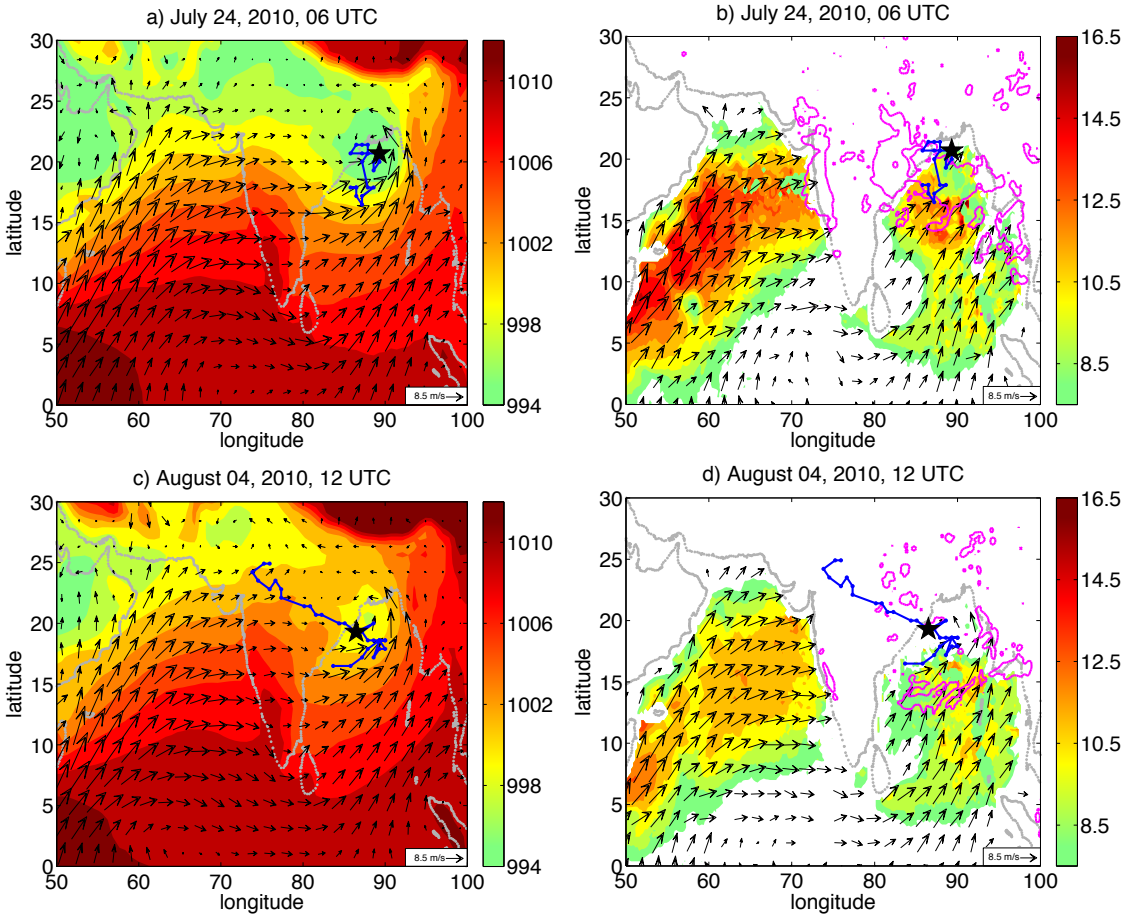

Supplemental Fig. 2 – Two monsoon depressions observed in the Yale and NYUAD datasets during the summer of 2010. In all panels storm tracks (from the Yale dataset) are shown by blue lines with vortex center marked with a black star. Left column: ERA-Interim sea-level pressure (in hPa) is shaded and black arrows show the ERA-Interim surface wind vector field. Right column: SSM/I surface wind speed is shaded, while arrows show surface wind vector from WindSat scatterometer. The thick magenta contour shows the 40 mm day^{-1} daily TRMM precipitation.

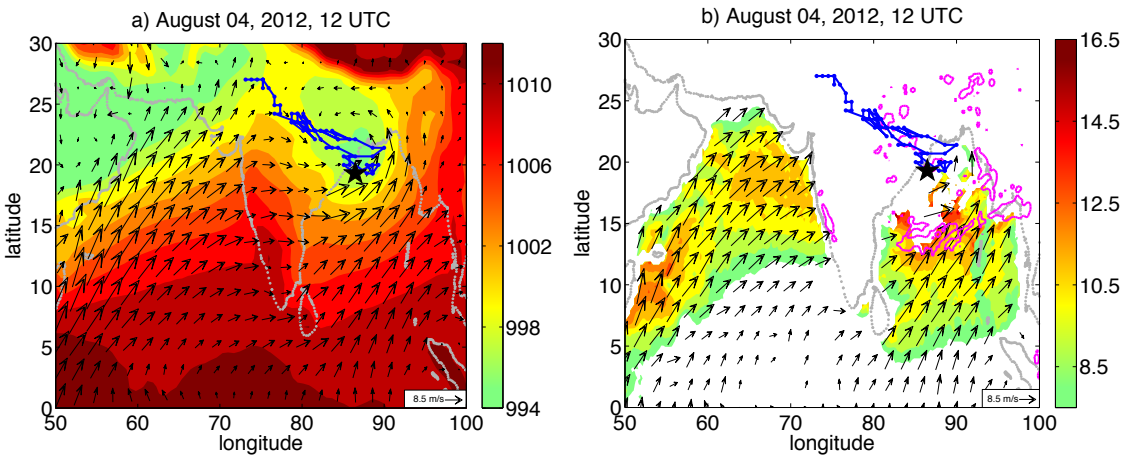

Supplemental Fig. 3 – A monsoon depression observed in the Yale and NYUAD datasets during the summer of 2012. In all panels storm tracks (from the Yale dataset) are shown by blue lines with vortex center marked with a black star. Left column: ERA-Interim sea-level pressure (in hPa) is shaded and black arrows show the ERA-Interim surface wind vector field. Right column: SSM/I surface wind speed is shaded, while arrows show surface wind vector from WindSat scatterometer. The thick magenta contour shows the 40 mm day^{-1} daily TRMM precipitation.

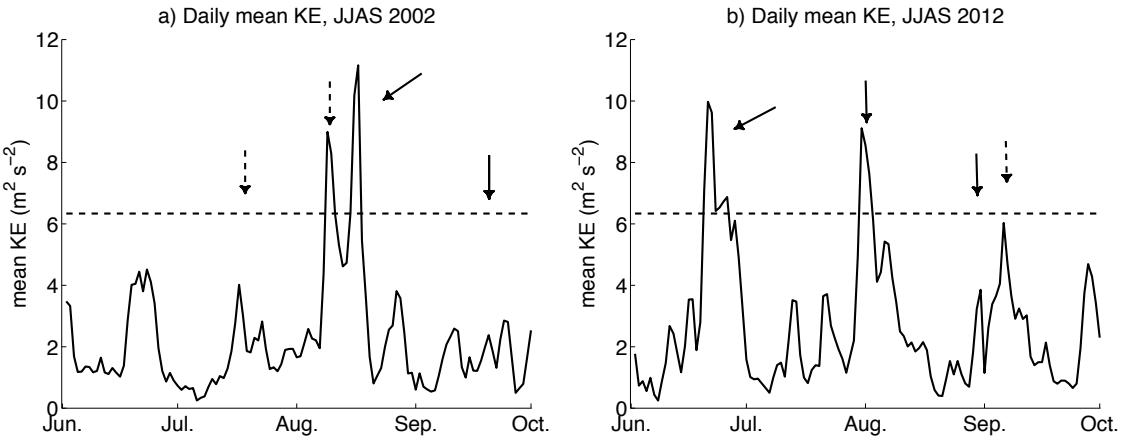

Supplemental Fig. 4 – The synoptic KE, using SSM/I data, as a function of time for the summers of 2002 and 2012. The 90th percentile threshold for extreme events is marked by the dashed line. Arrows correspond to monsoon lows (dashed) and monsoon depressions (solid) that took place roughly around the same time in the main genesis region of the Bay of Bengal domain (15-25°N and 80-100°E).

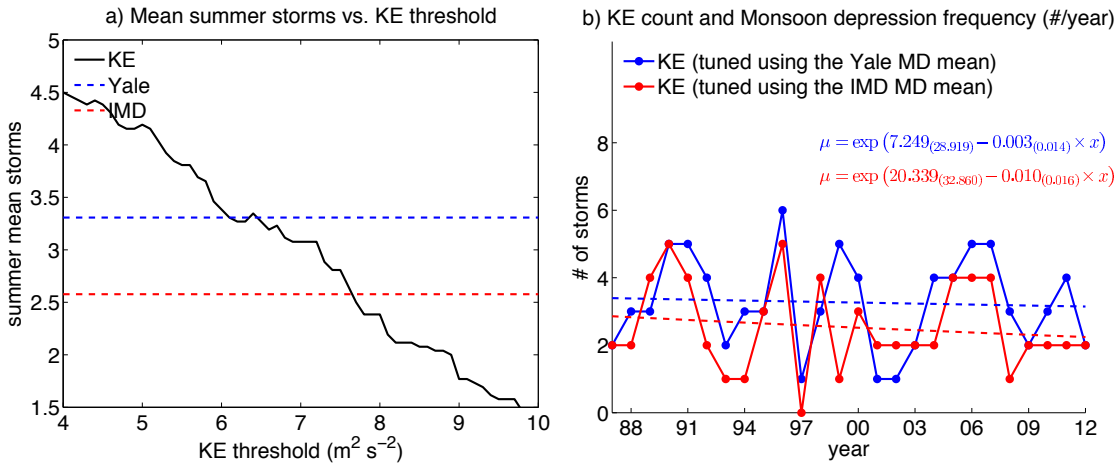

Supplemental Fig. 5 – Sensitivity test for the synoptic KE count. Panel (a) shows the summer mean synoptic KE storm count as a function the synoptic KE threshold. The dashed lines correspond to the summer mean monsoon depression in the Yale (blue) and IMD (red) datasets. The cross-cutting points are used in panel (b) to tune the synoptic KE threshold to produce KE count that will have the same summer mean as in the Yale and IMD datasets. In panel (b) the tuned KE counts are shown (solid lines). The nonlinear regression fits to the tuned KE counts are shown too (dashed lines).

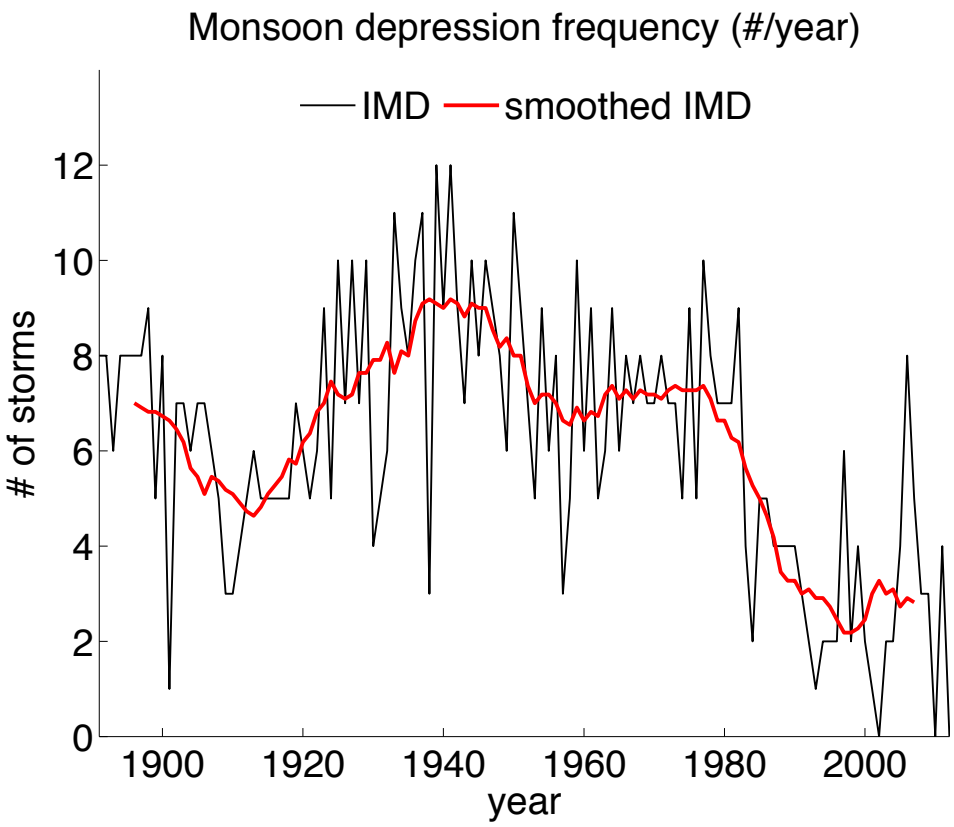

Supplemental Fig. 6 – Monsoon depression frequency over Bay of Bengal (5-27°N and 70-100°E) using the IMD dataset (black) for 1891-2012, and its smoothed trend using 11-year centered moving average (red).

Supplemental Table 1 – Linear and nonlinear Poisson regression fits to the datasets presented in Figs. 1b, 1c, 4c and 4d. The standard errors of each fit's coefficients are shown parenthetically below the coefficients themselves (multiply by 1.96 to get the 95% confidence interval).

Dataset	Linear and Nonlinear Poisson regression fit
IMD (Fig. 1b)	$\ln \mu = 65.342_{(19.092)} - 0.032_{(0.010)} \times x$
SIKKA (Fig. 1b)	$\ln \mu = 118.159_{(29.496)} - 0.059_{(0.015)} \times x$
ERA-Interim Yale (Fig. 1c)	$\ln \mu = -18.617_{(17.127)} + 0.010_{(0.009)} \times x$
MERAA NYUAD (Fig. 1c)	$\ln \mu = -16.012_{(12.824)} + 0.009_{(0.006)} \times x$
ERA-Interim NYUAD (Fig. 1c)	$\ln \mu = 19.632_{(14.303)} - 0.009_{(0.007)} \times x$
Averaged Reanalysis data (Fig. 1c)	$\ln \mu = -4.54_{(14.413)} + 0.003_{(0.007)} \times x$
KE (Figs. 4c and 4d)	$\ln \mu = 7.250_{(28.920)} - 0.003_{(0.015)} \times x$
ERA-Interim Yale (Fig. 4c)	$\ln \mu = -31.981_{(28.896)} + 0.017_{(0.014)} \times x$
IMD (Fig. 4c)	$\ln \mu = 22.330_{(32.614)} - 0.010_{(0.016)} \times x$
Summer average KE (Fig. 4d)	$\mu = 44.860_{(26.737)} - 0.021_{(0.013)} \times x$